NANO LETTERS

Letter

pubs.acs.org/NanoLett

Copper Nanocrystals Encapsulated in Zr-based Metal–Organic Frameworks for Highly Selective CO_2 Hydrogenation to Methanol

Bunyarat Rungtaweevoranit,[†,‡] Jayeon Baek,[†,‡] Joyce R. Araujo,[†,∥] Braulio S. Archanjo,[∥] Kyung Min Choi,[†,‡] Omar M. Yaghi,*[,†,‡,⊥] and Gabor A. Somorjai*[,†,§]

[†]Department of Chemistry, University of California–Berkeley, Kavli Energy NanoSciences Institute, Berkeley, California 94720, United States

[‡]Materials Sciences Division and [§]Chemical Sciences Division, Lawrence Berkeley National Laboratory, Berkeley, California 94720, United States

[∥]Materials Metrology Division, National Institute of Metrology, Quality, and Technology, Duque de Caxias, Rio de Janeiro 25250–020, Brazil

[⊥]King Abdulaziz City for Science and Technology, Riyadh 11442, Saudi Arabia

Supporting Information

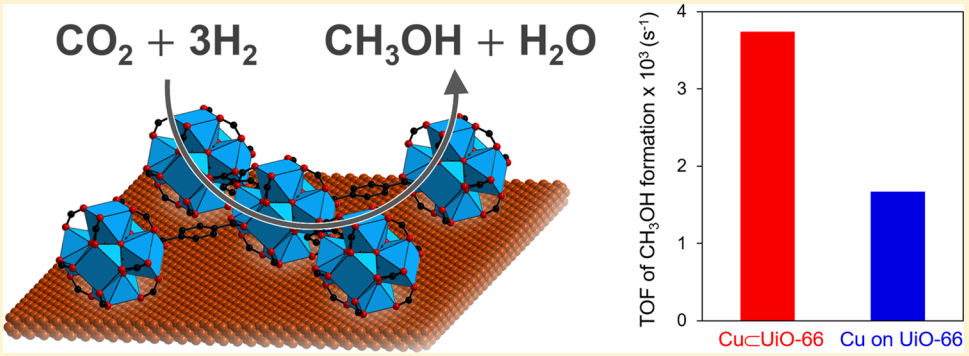

ABSTRACT: We show that the activity and selectivity of Cu catalyst can be promoted by a Zr-based metal–organic framework (MOF), $Zr_6O_4(OH)_4(BDC)_6$ (BDC = 1,4-benzenedicarboxylate), UiO-66, to have a strong interaction with Zr oxide $[Zr_6O_4(OH)_4(-CO_2)_{12}]$ secondary building units (SBUs) of the MOF for CO_2 hydrogenation to methanol. These interesting features are achieved by a catalyst composed of 18 nm single Cu nanocrystal (NC) encapsulated within single crystal UiO-66 (Cu⊂UiO-66). The performance of this catalyst construct exceeds the benchmark $Cu/ZnO/Al_2O_3$ catalyst and gives a steady 8-fold enhanced yield and 100% selectivity for methanol. The X-ray photoelectron spectroscopy data obtained on the surface of the catalyst show that Zr 3d binding energy is shifted toward lower oxidation state in the presence of Cu NC, suggesting that there is a strong interaction between Cu NC and Zr oxide SBUs of the MOF to make a highly active Cu catalyst.

KEYWORDS: *Metal–organic framework, metal nanocrystal, heterogeneous catalyst, CO_2 hydrogenation, methanol, strong metal–support interaction*

Methanol produced by hydrogenation of CO_2 is an attractive route to recycle the captured CO_2 from fossil fuel combustion sources.[1] It is a convenient fuel to transport as a hydrogen-rich source and it is also used as a chemical feedstock to produce other key chemical intermediates.[2] Currently, it is produced industrially from synthesis gas (a mixture of CO, CO_2, and H_2) using a $Cu/ZnO/Al_2O_3$ catalyst.[3] However, isotope labeling experiments revealed that CO_2 is the main carbon source for methanol production and CO is responsible for maintaining the active oxidation state of Cu.[4] Therefore, finding catalysts that use CO_2 and H_2 as the only sources to produce methanol selectively is desirable but remains a challenge.[5] For instance, CO has been observed as a byproduct from the reverse water–gas shift reaction, that is, $CO_2 + H_2 \rightleftharpoons CO + H_2O$, over $Cu/ZnO/Al_2O_3$ catalyst and newly discovered Ni–Ga heterogeneous catalyst as well.[6] More recently, "MnO_x"/mesoporous Co_3O_4 catalyst was used to produce the highest reported yield of methanol under mild temperature and pressure conditions (250 °C, 6 bar).[7] However, these catalysts suffer from lower selectivity as either hydrocarbons and/or CO are also produced along with methanol. Here, we report a catalyst composed of Cu nanocrystal (NC) encapsulated within a metal–organic framework (MOF) for the conversion of CO_2 to methanol with 100% selectivity and high activity.

Received: August 29, 2016
Revised: October 26, 2016
Published: November 2, 2016

DOI: 10.1021/acs.nanolett.6b03637
Nano Lett. 2016, 16, 7645–7649

CO_2 hydrogenation to methanol reaction is generally known to be structure sensitive in that the catalytic properties are strongly associated with the dimension and composition of the metal oxide−metal interface.[8] MOFs are advantageous in this regard for interfacing with other catalytically active metal because of their nanosized metal oxide secondary building units (SBUs) and tunability of their compositions; hence allowing us to investigate the effects of catalytic interface systematically.[9]

Specifically, we report a catalyst where Cu NC is encapsulated inside a Zr(IV)-based MOF denoted as Cu⊂UiO-66, UiO-66 [$Zr_6O_4(OH)_4(BDC)_6$, BDC = 1,4-benzenedicarboxylate][10] (Scheme 1), for CO_2 hydrogenation to methanol. In this construct, an ordered array of Zr oxide SBUs are precisely placed on the Cu surface yielding high interfacial contact between Cu NC and Zr oxide SBUs. Furthermore, these Zr oxide SBUs are spatially spaced by organic linkers ensuring the accessibility of reactants to the active sites. We found that Cu⊂UiO-66 shows 8-fold enhanced catalytic activity in comparison to the benchmark $Cu/ZnO/Al_2O_3$ catalyst[11] while maintaining 100% selectivity toward methanol.

Scheme 1. Crystal Structure of UiO-66 Where Zr Oxide SBUs Are Linked with BDC To Form an Ordered Array of the SBUs[a]

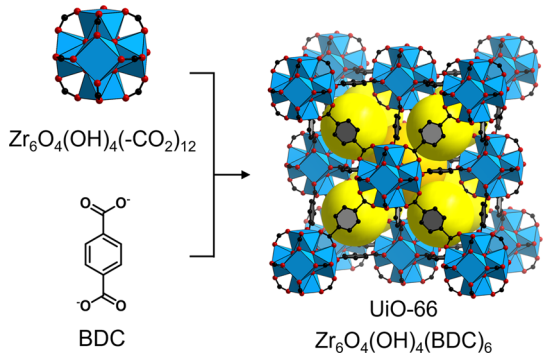

[a]Atom labeling scheme: C, black; O, red; Zr, blue polyhedra. H atoms are omitted for clarity. Yellow spheres represent the space in the framework.

Synthesis and Characterization of Cu NC within (Cu⊂UiO-66) and on UiO-66 (Cu on UiO-66). We developed the synthesis procedure for 18 nm Cu NCs capped polyvinylpyrrolidone (PVP) using polyol process and they were used throughout this study [see Supporting Information (SI), Figure S1]. This permitted us to systematically study the change in the catalytic properties as a function of various MOFs and other supports. For Cu⊂UiO-66, the presynthesized Cu NCs were added to the solution containing the MOF precursors. In addition to the exclusion of oxygen to prevent the surface oxidation and subsequent acid-mediated dissolution of Cu NCs,[12] we observed that the choice of metal precursors dramatically affected the encapsulation process. Typical Zr precursors for the synthesis of UiO-66 are $ZrOCl_2{\cdot}8H_2O$ and $ZrCl_4$, which led to the dissolution of Cu NCs.[13] We found that the use of $Zr(OPr^n)_4$ led to the successful production of Cu⊂UiO-66 as single Cu inside single nanocrystalline UiO-66 (Figure 1A). This material is the first example of Cu NCs being encapsulated inside the framework as a well-defined construct.[14] For Cu NCs immobilized on UiO-66 (Cu on UiO-66), we deposited Cu NCs on the presynthesized UiO-66 by mixing colloidal solutions of Cu NCs and UiO-66 where UiO-66 was prepared using $Zr(OPr^n)_4$ as well (Figure 1B).

The catalysts were further characterized by powder X-ray diffraction (PXRD), N_2 adsorption−desorption isotherms, and inductively coupled plasma atomic emission spectroscopy (ICP-AES). The Cu NC-MOF constructs display diffraction lines that coincide with the simulated patterns confirming the crystallinity and identity of the materials (Figure 1C). N_2 adsorption isotherms show that all the materials are porous (Figure 1D) and ICP-AES measurements indicate 1 and 1.4 wt % of Cu for Cu⊂UiO-66 and Cu on UiO-66, respectively (SI, Table S1).

CO_2 Hydrogenation to Methanol. We first studied the catalytic properties of Cu NCs integrated with various MOFs and conventional supports. We tested three MOFs with different SBUs namely UiO-66 with a Zr oxide SBU, MIL-101 (Cr) [$Cr_3O(H_2O)_2(BDC)_3(OH)$] with a Cr oxide SBU,[15] and ZIF-8 [$Zn(C_4H_5N_2)_2$] with a Zn−N SBU (SI, Figures S2 and S3).[16] We also tested Cu NCs supported on traditional supports, mesoporous silica (MCF-26), ZrO_2, and Al_2O_3, as they are commonly known to be either inert or active supports for this reaction. For comparison, $Cu/ZnO/Al_2O_3$ catalyst was used as a benchmark reference and tested under the same reaction condition.[17]

CO_2 hydrogenation at 175 °C and 10 bar using CO_2 and H_2 in a 1:3 molar ratio revealed that only Cu⊂UiO-66, Cu on UiO-66, Cu on ZrO_2, and $Cu/ZnO/Al_2O_3$ can convert CO_2 to methanol with an initial turnover frequency (TOF) of methanol formation of 3.7×10^{-3}, 1.7×10^{-3}, 0.42×10^{-3}, and 0.45×10^{-3} s^{-1}, respectively. Neither Cu NCs on MIL-101 (Cr) nor Cu NCs⊂ZIF-8 show catalytic activity. These results indicate that only the materials containing Zr oxide or Zn oxide in either cluster or nanocrystal form can catalyze CO_2 hydrogenation to methanol. Furthermore, it is remarkable that Zr oxide SBUs of UiO-66 can function as ZrO_2 or even better in promoting Cu catalyst.

The difference in catalytic activity can be attributed to the variations in the composition of the SBUs and not from variations in the structural stability. We examined the structural integrity of the MOF-based catalysts after the reactions by TEM, PXRD, and N_2 adsorption−desorption measurements (SI, Section S2). The crystallinity and porosity of UiO-66, MIL-101 (Cr), and ZIF-8 were preserved throughout the reaction. From the elemental analysis (EA), ^1H NMR, and TGA measurement results, we do not observe coking deposited inside the catalysts (SI, Section S2).

Figure 2 displays the initial TOF of methanol formation over Cu⊂UiO-66 in comparison with Cu on UiO-66 catalysts. By comparing the catalysis activity between Cu⊂UiO-66 and Cu on UiO-66, we find that the location of the Cu NC also influences the catalytic activity. Cu⊂UiO-66 catalyst shows a 2-fold increase and much enhanced stability in activity (SI, Figure S18) presumably due to the higher number of contact points between the Zr oxide SBU and Cu surface and the confinement of the Cu NC in the MOF.[18] This result implies that the Cu NC environment surrounded by the Zr oxide SBU can help in creating active Cu sites for catalytic conversion of CO_2 to methanol.

We increased the reaction temperature to 200 °C, 225 °C, and 250 °C at 10 bar to observe the thermodynamic effect under low conversion (below the diffusion limit). The CO_2 hydrogenation to methanol is an exothermic reaction ($CO_2 + 3H_2 \rightleftharpoons CH_3OH + H_2O$, $\Delta H^\circ = -49.4$ kJ mol^{-1}) whereas the

DOI: 10.1021/acs.nanolett.6b03637
Nano Lett. 2016, 16, 7645−7649

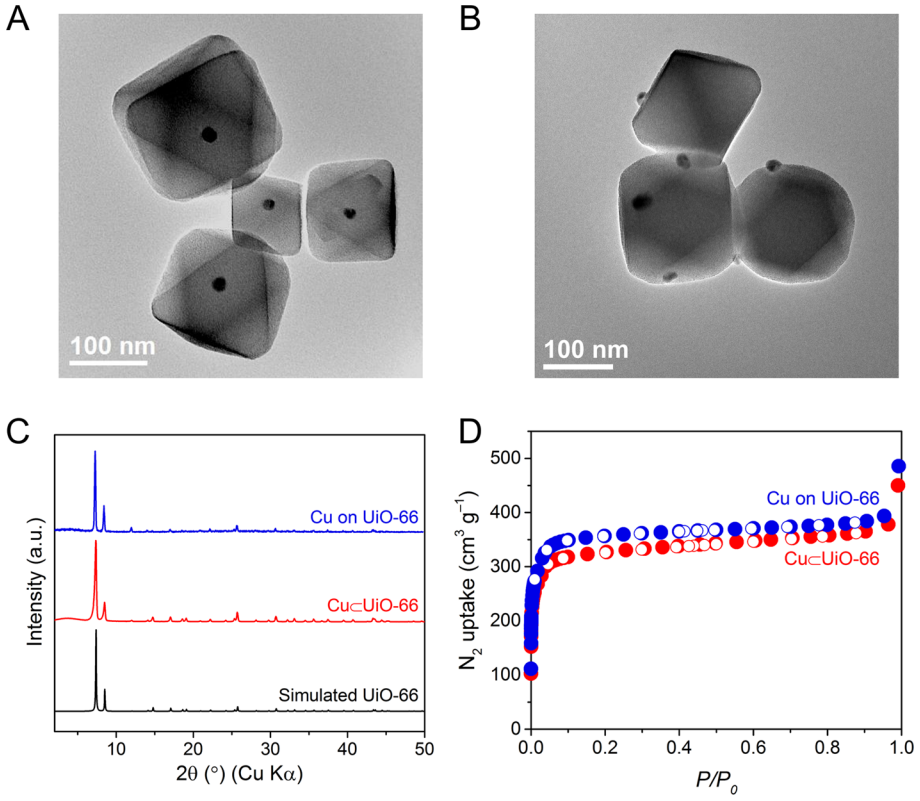

Figure 1. Characterization of Cu decorated MOFs: TEM images of (A) Cu⊂UiO-66 (single Cu NC inside UiO-66), (B) Cu on UiO-66, (C) experimental PXRD patterns in comparison with simulated pattern from single crystal X-ray diffraction data, and (D) N_2 adsorption−desorption isotherms at 77 K with adsorption and desorption points represented by closed circles and open circles, respectively (P/P_0, relative pressure).

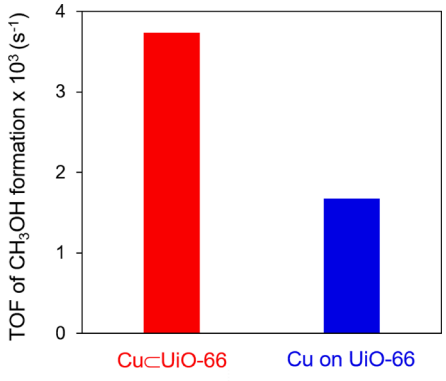

Figure 2. Initial TOFs of methanol formation over Cu⊂UiO-66 and Cu on UiO-66. The reaction rates were measured after 1 h. Reaction conditions: 7 sccm of CO_2, 21 sccm of H_2, 10 bar, and 175 °C.

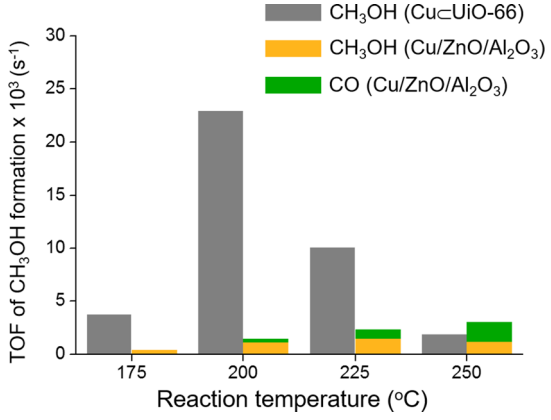

Figure 3. TOFs of product formation over Cu⊂UiO-66 catalyst and $Cu/ZnO/Al_2O_3$ catalyst as various reaction temperatures. No CO is produced in the case of Cu⊂UiO-66 under all reaction temperatures.

reverse water−gas shift reaction is endothermic ($CO_2 + H_2 \rightleftharpoons CO + H_2O$, ΔH° = +41.2 kJ mol^{-1}), therefore the CO production is favored at higher temperature.[17] Figure 3 indicates the initial TOF of product formation at four different reaction temperatures for Cu⊂UiO-66 and $Cu/ZnO/Al_2O_3$. As the reaction temperature increases, the TOF of CO formation steeply increases in the benchmark $Cu/ZnO/Al_2O_3$ catalyst [selectivity for CO = 0% (175 °C), 33% (200 °C), 42% (225 °C), and 61% (250 °C)]. Interestingly, no CO was detected in the Cu⊂UiO-66 catalyst at all reaction temperatures. This high methanol selectivity of Cu⊂UiO-66 is not due to the low CO_2 conversion but the intrinsic property of the catalyst because Cu⊂UiO-66 and $Cu/ZnO/Al_2O_3$ showed similar conversion (~5%) at 200 °C (SI, Figure S20 and S21).

At four different reaction temperatures, the initial TOF of methanol formation over Cu⊂UiO-66 always outperforms $Cu/ZnO/Al_2O_3$. We found that the optimal reaction temperature for Cu⊂UiO-66 is 175 °C as it shows stable catalytic activity (SI, Figures S23 and S24). At this reaction temperature, Cu⊂UiO-66 exhibits 8-fold enhancement of catalytic activity in comparison to $Cu/ZnO/Al_2O_3$.

X-ray Photoelectron Spectroscopy (XPS) Analysis. To understand the origin of high activity and high selectivity of Cu⊂UiO-66, we performed XPS analysis to probe the electronic properties of the catalyst. However, the distance

DOI: 10.1021/acs.nanolett.6b03637
Nano Lett. 2016, 16, 7645−7649

between the Cu NC and the surface of the Cu⊂UiO-66 crystal is beyond the penetration depth of the X-rays used in XPS.[19] We then turned to investigate Cu on UiO-66 and used it as a proxy for Cu⊂UiO-66. We believe this is reasonable because Cu on UiO-66 also shows 100% selectivity for methanol and comparable activity and therefore most likely have the same active catalyst interface.

Despite the use of as-synthesized Cu on UiO-66 catalyst, Cu was readily oxidized under ambient condition, the surface oxidation state of the Cu NC is Cu(II) as shown by the 934 eV binding energy in the XPS Cu 2p spectrum (SI, Figure S25).[20] This is presumably due to surface oxidation of Cu NCs to form a $Cu/Cu_2O/CuO$ structure as reported previously.[21] The Zr $3d_{5/2}$ spectrum in UiO-66 without Cu exhibits binding energy of 182.8 eV that corresponds to the Zr(IV) oxidation state in the Zr oxide SBU $[Zr_6O_4(OH)_4(-CO_2)_{12}]$.[22] In the case of the Zr 3d spectrum of Cu on UiO-66 catalyst, the Zr $3d_{5/2}$ peak shift from 182.8 to 182.2 eV was observed, highlighting that the Zr(IV) is reduced when in contact with the Cu NCs (Figure 4A).[23] The fact that Zr(IV) in UiO-66 is reduced implies that Cu is oxidized inherently.

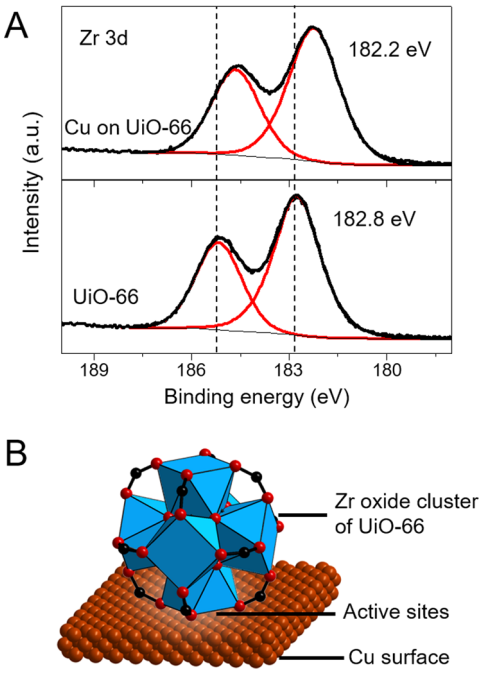

Figure 4. (A) XPS Zr 3d spectra of UiO-66 and Cu on UiO-66. (B) Illustration of active site of Cu NC-UiO-66 catalyst. One Zr oxide SBU $[Zr_6O_4(OH)_4(-CO_2)_{12}]$ is used as a representative of ordered array of SBUs. Atom labeling scheme: Cu, brown; C, black; O, red; Zr, blue polyhedra. H atoms are omitted for clarity.

These changes in the oxidation state of Zr suggest the interaction between Cu NC and Zr oxide SBU, also known as a strong metal−support interaction effect. Considering this effect, Cu NC in contact with UiO-66 would result in the combination of metallic Cu and Cu cation species even after the reduction. The combination of Cu species positively affects the reaction because each species cooperatively play a role during the catalysis: (i) hydrogen dissociation by metallic Cu species,[3,24] and (ii) stabilization of the intermediates (i.e., formate) by cationic Cu species.[5c] It is generally accepted that dissociation of the hydrogen molecule is fast and the hydrogenation of surface formate is the rate-determining step.[25] Thus, the presence of copper cationic species after reduction is necessary. On the basis of these observations, we postulate that the active site for the Cu NC−UiO-66 catalyst is the interface between Cu NC and Zr oxide SBU $[Zr_6O_4(OH)_4(-CO_2)_{12}]$ (Figure 4B).

In contrast to the previous report on Cu/ZrO_2 where Zr $3d_{5/2}$ peak shift was not detected despite the presence of the interaction between Cu and ZrO_2, the peak shift of Zr oxide SBU observed here suggests the higher interfacial contact area between Zr oxide SBU and Cu NC.[26] This effect can be attributed to the nanosized metal oxide SBU in the MOF backbone.

In summary, the support effect on the Cu catalyst for the CO_2 hydrogenation to methanol was investigated over different types of MOFs [UiO-66, MIL-101 (Cr), and ZIF-8], mesoporous silica (MCF-26), ZrO_2, and Al_2O_3. We found that UiO-66 is the best promoter for Cu catalyst giving high selectivity and high yield for the production of methanol from CO_2. From XPS analysis and catalytic experiments, we believe that the presence of the combination of multiple Cu oxidation states and the higher interfacial contact area between Cu NCs and Zr oxide SBUs of the MOF lead to the high TOF for methanol formation. To our knowledge, this is the first finding that metal oxide clusters (SBU) in MOF can have strong-metal support interaction as typically observed in bulk metal oxides.

■ ASSOCIATED CONTENT

Supporting Information

The Supporting Information is available free of charge on the ACS Publications website at DOI: 10.1021/acs.nanolett.6b03637.

Detailed information on synthesis of catalysts, materials characterization, and catalysis (PDF)

■ AUTHOR INFORMATION

Corresponding Authors

*E-mail: yaghi@berkeley.edu.
*E-mail: somorjai@berkeley.edu.

Author Contributions

B.R. and J.B. contributed equally.

Notes

The authors declare no competing financial interest.

■ ACKNOWLEDGMENTS

G.A.S. acknowledges support from the Director, Office of Basic Energy Sciences, Division of Chemical Sciences, Geological and Biosciences of the U.S. Department of Energy under contract No. DEAC02-05CH11231. O.M.Y. thanks BASF SE (Ludwigshafen, Germany), U.S. Department of Defense, Defense Threat Reduction Agency (HDTRA 1-12-1-0053), and King Abdulaziz City for Science and Technology (Riyadh, Saudi Arabia) for financial support. NMR, TEM, and XPS measurements were performed at the Molecular Foundry, which was supported by the Office of Science, Office of Basic Energy Sciences, of the DOE under Contract No. DE-AC02-05CH11231. We thank Dr. Juncong Jiang (Yaghi group) for providing MIL-101 (Cr) sample and Drs. Peter Siman, Gérôme Melaet, Kairat Sabyrov, and Mr. Walter T. Ralston for useful discussions. B.R. is supported by the Royal Thai Government Scholarship. J.R.A. and B.S.A. acknowledge CNPq for their fellowships 234217/2014-6.

DOI: 10.1021/acs.nanolett.6b03637
Nano Lett. 2016, 16, 7645−7649

REFERENCES

(1) (a) Schoedel, A.; Ji, Z.; Yaghi, O. M. *Nat. Energy* **2016**, *1*, 16034. (b) Goeppert, A.; Czaun, M.; Jones, J.-P.; Surya Prakash, G. K.; Olah, G. A. *Chem. Soc. Rev.* **2014**, *43*, 7995.

(2) Stöcker, M. *Microporous Mesoporous Mater.* **1999**, *29*, 3.

(3) Behrens, M.; Studt, F.; Kasatkin, I.; Kühl, S.; Hävecker, M.; Abild-Pedersen, F.; Zander, S.; Girgsdies, F.; Kurr, P.; Kniep, B.-L.; Tovar, M.; Fischer, R. W.; Nørskov, J. K.; Schlögl, R. *Science* **2012**, *336*, 893.

(4) (a) Chinchen, G. C.; Denny, P. J.; Jennings, J. R.; Spencer, M. S.; Waugh, K. C. *Appl. Catal.* **1988**, *36*, 1. (b) Chinchen, G. C.; Denny, P. J.; Parker, D. G.; Spencer, M. S.; Whan, D. A. *Appl. Catal.* **1987**, *30*, 333.

(5) (a) Graciani, J.; Mudiyanselage, K.; Xu, F.; Baber, A. E.; Evans, J.; Senanayake, S. D.; Stacchiola, D. J.; Liu, P.; Hrbek, J.; Sanz, J. F.; Rodriguez, J. A. *Science* **2014**, *345*, 546. (b) Martin, O.; Martín, A. J.; Mondelli, C.; Mitchell, S.; Segawa, T. F.; Hauert, R.; Drouilly, C.; Curulla-Ferré, D.; Pérez-Ramírez, J. *Angew. Chem., Int. Ed.* **2016**, *55*, 6261. (c) Liu, C.; Yang, B.; Tyo, E.; Seifert, S.; DeBartolo, J.; von Issendorff, B.; Zapol, P.; Vajda, S.; Curtiss, L. A. *J. Am. Chem. Soc.* **2015**, *137*, 8676.

(6) Studt, F.; Sharafutdinov, I.; Abild-Pedersen, F.; Elkjær, C. F.; Hummelshøj, J. S.; Dahl, S.; Chorkendorff, I.; Nørskov, J. K. *Nat. Chem.* **2014**, *6*, 320.

(7) Li, C.-S.; Melaet, G.; Ralston, W. T.; An, K.; Brooks, C.; Ye, Y.; Liu, Y.-S.; Zhu, J.; Guo, J.; Alayoglu, S.; Somorjai, G. A. *Nat. Commun.* **2015**, *6*, 6538.

(8) Grabow, L. C.; Mavrikakis, M. *ACS Catal.* **2011**, *1*, 365.

(9) (a) Choi, K. M.; Na, K.; Somorjai, G. A.; Yaghi, O. M. *J. Am. Chem. Soc.* **2015**, *137*, 7810. (b) Rösler, C.; Fischer, R. A. *CrystEngComm* **2015**, *17*, 199. (c) Hu, P.; Morabito, J. V.; Tsung, C.-K. *ACS Catal.* **2014**, *4*, 4409. (d) Furukawa, H.; Cordova, K. E.; O'Keeffe, M.; Yaghi, O. M. *Science* **2013**, *341*, 1230444. (e) Rungtaweevoranit, B.; Zhao, Y.; Choi, K. M.; Yaghi, O. M. *Nano Res.* **2016**, *9*, 47. (f) Na, K.; Choi, K. M.; Yaghi, O. M.; Somorjai, G. A. *Nano Lett.* **2014**, *14*, 5979.

(10) Cavka, J. H.; Jakobsen, S.; Olsbye, U.; Guillou, N.; Lamberti, C.; Bordiga, S.; Lillerud, K. P. *J. Am. Chem. Soc.* **2008**, *130*, 13850.

(11) Wang, W.; Wang, S.; Ma, X.; Gong, J. *Chem. Soc. Rev.* **2011**, *40*, 3703.

(12) (a) Kuo, C.-H.; Tang, Y.; Chou, L.-Y.; Sneed, B. T.; Brodsky, C. N.; Zhao, Z.; Tsung, C.-K. *J. Am. Chem. Soc.* **2012**, *134*, 14345. (b) Hung, L.-I.; Tsung, C.-K.; Huang, W.; Yang, P. *Adv. Mater.* **2010**, *22*, 1910.

(13) Tulig, K.; Walton, K. S. *RSC Adv.* **2014**, *4*, 51080.

(14) (a) Hu, P.; Zhuang, J.; Chou, L.-Y.; Lee, H. K.; Ling, X. Y.; Chuang, Y.-C.; Tsung, C.-K. *J. Am. Chem. Soc.* **2014**, *136*, 10561. (b) Luz, I.; Loiudice, A.; Sun, D. T.; Queen, W. L.; Buonsanti, R. *Chem. Mater.* **2016**, *28*, 3839. (c) Müller, M.; Hermes, S.; Kähler, K.; van den Berg; Maurits, W. E.; Muhler, M.; Fischer, R. A. *Chem. Mater.* **2008**, *20*, 4576.

(15) Férey, G.; Mellot-Draznieks, C.; Serre, C.; Millange, F.; Dutour, J.; Surblé, S.; Margiolaki, I. *Science* **2005**, *309*, 2040.

(16) Park, K. S.; Ni, Z.; Côté, A. P.; Choi, J. Y.; Huang, R.; Uribe-Romo, F. J.; Chae, H. K.; O'Keeffe, M.; Yaghi, O. M. *Proc. Natl. Acad. Sci. U. S. A.* **2006**, *103*, 10186.

(17) There is no significant size-dependent catalytic activity in this Cu particle size regime, 18 nm for Cu NC for Cu⊂UiO-66 and ∼ 10 nm for Cu/ZnO/Al_2O_3. Arena, F.; Barbera, K.; Italiano, G.; Bonura, G.; Spadaro, L.; Frusteri, F. *J. Catal.* **2007**, *249*, 185.

(18) Joo, S. H.; Park, J. Y.; Tsung, C.-K.; Yamada, Y.; Yang, P.; Somorjai, G. A. *Nat. Mater.* **2009**, *8*, 126.

(19) Alayoglu, S.; Beaumont, S. K.; Zheng, F.; Pushkarev, V. V.; Zheng, H.; Iablokov, V.; Liu, Z.; Guo, J.; Kruse, N.; Somorjai, G. A. *Top. Catal.* **2011**, *54*, 778.

(20) For XPS binding energy information, see: Duke, A. S.; Dolgopolova, E. A.; Galhenage, R. P.; Ammal, S. C.; Heyden, A.; Smith, M. D.; Chen, D. A.; Shustova, N. B. *J. Phys. Chem. C* **2015**, *119*, 27457.

(21) Yin, M.; Wu, C.-K.; Lou, Y.; Burda, C.; Koberstein, J. T.; Zhu, Y.; O'Brien, S. *J. Am. Chem. Soc.* **2005**, *127*, 9506.

(22) Long, J.; Wang, S.; Ding, Z.; Wang, S.; Zhou, Y.; Huang, L.; Wang, X. *Chem. Commun.* **2012**, *48*, 11656.

(23) Lewera, A.; Timperman, L.; Roguska, A.; Alonso-Vante, N. *J. Phys. Chem. C* **2011**, *115*, 20153.

(24) Kiennemann, A.; Hindermann, J. P. *Stud. Surf. Sci. Catal.* **1988**, *35*, 181.

(25) Yang, Y.; Mims, C. A.; Mei, D. H.; Peden, C.; Campbell, C. T. *J. Catal.* **2013**, *298*, 10.

(26) Samson, K.; Śliwa, M.; Socha, R. P.; Góra-Marek, K.; Mucha, D.; Rutkowska-Zbik, D.; Paul, J.-F.; Ruggiero-Mikołajczyk, M.; Grabowski, R.; Słoczyński, J. *ACS Catal.* **2014**, *4*, 3730.

DOI: 10.1021/acs.nanolett.6b03637
Nano Lett. 2016, 16, 7645−7649